



Synthetic Communications

An International Journal for Rapid Communication of Synthetic Organic Chemistry

ISSN: 0039-7911 (Print) 1532-2432 (Online) Journal homepage: <https://www.tandfonline.com/loi/lcyc20>

Ultrasound assisted rapid synthesis, biological evaluation, and molecular docking study of new 1,2,3-triazolyl pyrano[2,3-c]pyrazoles as antifungal and antioxidant agent

Smita P. Khare, Tejshri R. Deshmukh, Jaiprakash N. Sangshetti, Vijay M. Khedkar & Bapurao B. Shingate

To cite this article: Smita P. Khare, Tejshri R. Deshmukh, Jaiprakash N. Sangshetti, Vijay M. Khedkar & Bapurao B. Shingate (2019): Ultrasound assisted rapid synthesis, biological evaluation, and molecular docking study of new 1,2,3-triazolyl pyrano[2,3-c]pyrazoles as antifungal and antioxidant agent, *Synthetic Communications*, DOI: [10.1080/00397911.2019.1631849](https://doi.org/10.1080/00397911.2019.1631849)

To link to this article: <https://doi.org/10.1080/00397911.2019.1631849>



Published online: 10 Jul 2019.



Submit your article to this journal [↗](#)



View Crossmark data [↗](#)



Ultrasound assisted rapid synthesis, biological evaluation, and molecular docking study of new 1,2,3-triazolyl pyrano[2,3-c]pyrazoles as antifungal and antioxidant agent

Smita P. Khare^a, Tejshri R. Deshmukh^a, Jaiprakash N. Sangshetti^b,
Vijay M. Khedkar^c, and Bapurao B. Shingate^a

^aDepartment of Chemistry, Dr. Babasaheb Ambedkar Marathwada University, Aurangabad, MH, India;

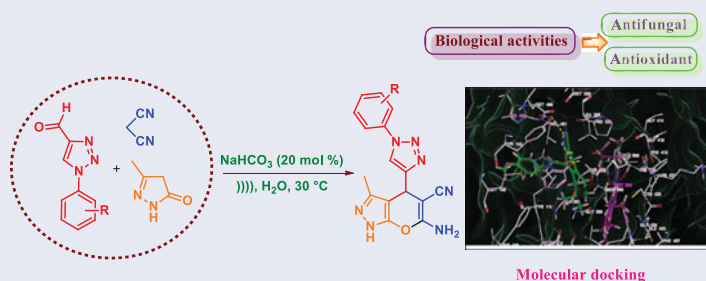
^bDepartment of Pharmaceutical Chemistry, Y. B. Chavan College of Pharmacy, Aurangabad, MH, India;

^cDepartment of Pharmaceutical Chemistry, Shri Vile Parle Kelavani Mandal's Institute of Pharmacy, Dhule, MH, India

ABSTRACT

In search of new generation of triazole based antifungal agents, synthesis of series of new 1,2,3-triazolyl pyrano[2,3-c]pyrazoles under ultrasonic irradiation using NaHCO₃ has been reported. The bioevaluation results indicate that, the compounds **7c**, **7d**, **7e**, **7f**, and **7i** displayed excellent antifungal activity with lower MIC $\leq 25 \mu\text{g/mL}$. Most of the compounds from the series showed potent antioxidant activity with a lower IC₅₀ value in the range 09.39 ± 0.42 – $14.97 \pm 0.24 \mu\text{g/mL}$, in comparison to butylated hydroxyl toluene (BHT). Molecular docking studies against potential target sterol 14 α -demethylase (CYP51) was also performed and showed excellent binding affinity with the target enzyme. Moreover, *in silico* ADME study shows that the derivatives could serve as drug like molecules for further drug development in clinical research.

GRAPHICAL ABSTRACT



ARTICLE HISTORY

Received 11 March 2019

KEYWORDS

Antifungal activity;
molecular docking study;
multicomponent reactions;
pyrano[2,3-c]pyrazole;
1,2,3-triazole

Introduction

Over the past few decades, invasive fungal infections among the immunocompromised and critically ill patients are growing rapidly and is becoming a leading cause of

CONTACT Bapurao B. Shingate  bapushingate@gmail.com  Department of Chemistry, Dr. Babasaheb Ambedkar Marathwada University, Aurangabad, 431 004, MH, India.

 Supplemental data for this article is available online at on the [publisher's website](#).

Color versions of one or more of the figures in the article can be found online at www.tandfonline.com/lsyc.

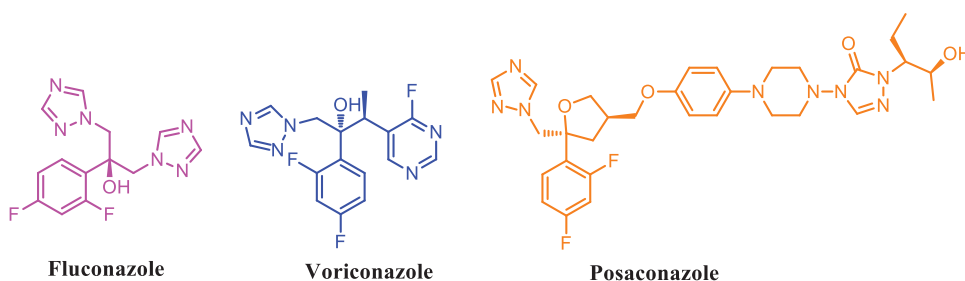


Figure 1. Azole based antifungal drugs.

morbidity and mortality.^[1] The high mortality rate was observed due to fungal infections caused by *Candida albicans* and *Cryptococcus neoformans*.^[2] The treatment of fungal infections becomes more difficult due to the decrease in efficiency of present azole-based drugs and developed resistance in most of the fungal strains. Clinically approved azole-based first-line drugs for the treatment of invasive fungal infections includes Fluconazole, Voriconazole, Posaconazole, and Itraconazole, etc. (Figure 1).^[3] Azole based antifungal agents target lanosterol 14 α -demethylase (CYP51) which is the key enzyme for the biosynthesis of ergosterol. The CYP51 enzyme catalyzes oxidative removal of 14 α -methyl group of lanosterol by monooxygenase activity. Azoles disrupt this oxidative removal through binding of azole N-4 to iron protoporphyrin unit of CYP51 which results in depletion of ergosterol and accumulation of 14 α -methylated sterol. This affects the membrane fluidity and activity of membrane enzymes which inhibits fungal growth.^[4]

1,2,3-Triazole nucleus has been reported as an important pharmacophoric scaffold, which is known to possess diverse biological activities.^[5] Along with the pharmacological profile, triazole nucleus possesses interesting physicochemical properties such as triazole moiety stable to acid–base hydrolysis, oxidation-reduction, capable to form H–bonding interaction, which helps to bind with biological targets. There are several reports on the synthesis of triazole-based molecules as antifungal,^[6] antitubercular,^[7] anticancer,^[8] antimicrobial,^[9] antiproliferative,^[10] anti-coronavirus,^[11] antibacterial,^[12] and neuroprotective agents.^[13] Some of the triazole-based drugs available in the market are Tazobactam, Cefatrizine and some are in the phases of clinical trials like CAI (Carboxyamidotriazole) (Figure 2).^[14]

On the other hand, pyrazole is one of the privileged *N*-heterocyclic scaffolds in medicinal research.^[15] Pyrazole and its derivatives possess a broad spectrum of biological activities, for instance, antifungal,^[16] anti-inflammatory,^[17] antihyperglycemic,^[18] antimicrobial,^[19] and antimalarial activities.^[20] There are a number of pyrazole containing drugs such as Celecoxib, Phenylbutazone, Pyrazomycine, Rimonabant, Apixaban, and Pyrazofurin available in the market (Figure 3).^[21]

4*H*-Pyran and pyran annulated heterocycles are observed in both nature and synthetic origin. Many pyran scaffolds are known to exhibit several biological activities^[22] and some of the biologically active synthetic 4*H*-pyran derivatives are shown in Figure 4.

4*H*-Pyran and its derivatives have been synthesized with much attention due to its biological significance. Several methods have been reported in the literature for the synthesis of pyrano[2,3-*c*]pyrazole^[23] through multicomponent reactions (MCRs).

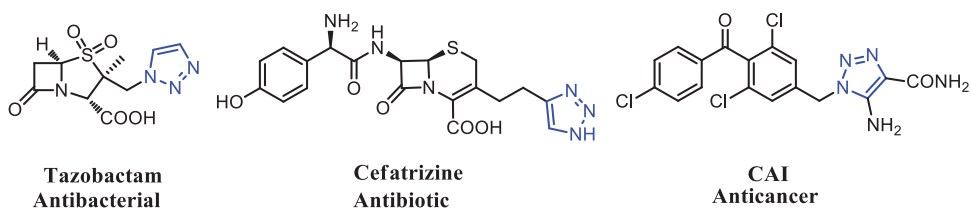


Figure 2. 1,2,3-Triazole based marketed drugs.

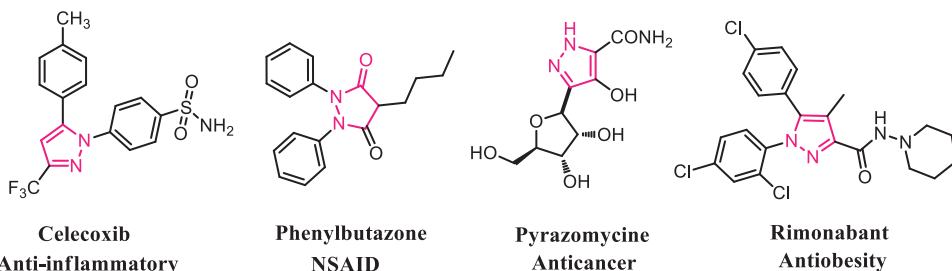


Figure 3. Medically important pyrazole based drug molecules.

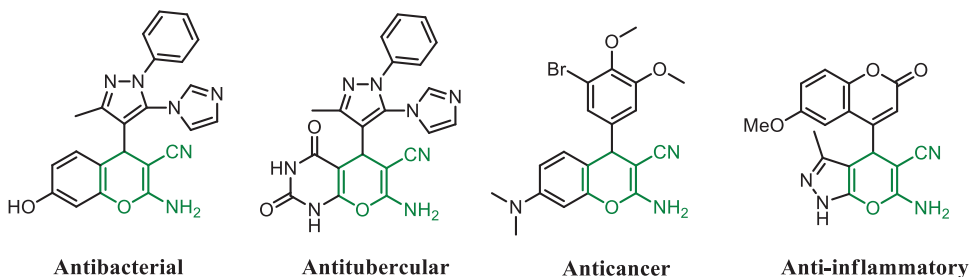


Figure 4. Biologically active 4H-Pyran derivatives.

In addition, their synthesis has also been reported by non-conventional techniques such as microwave irradiation, ultrasonic irradiation, and ball milling technique.^[24] However, most of these methods are useful with their own merits and demerits; yet, there is major scope for the development of newer green and efficient strategies for the synthesis of 4H-pyran and its derivatives.

Multicomponent reactions (MCRs) are one of the advantageous tools for the generation of diversified heterocyclic scaffolds in a single transformation.^[25] In addition to this, water-mediated MCRs is one of the greener approaches which helps in the development of economic and eco-friendly methodologies.^[26] Furthermore, ultrasonic irradiation (USI) is a green energy source which offers high yields in shorter reaction time.^[27] The mechanism of reaction under USI is based on acoustic cavitation effect with the formation and collapse of bubbles. This process generates high temperature and pressure in microseconds that lead to rate acceleration of reaction as compared to the traditional methods.

Impressed by the binding efficiency of 1,2,3-triazoles, pharmacological profile of pyrazole and pyran moieties discussed above, and in continuation of our research work on development of green synthetic methods, synthesis and evaluation of new heterocyclic

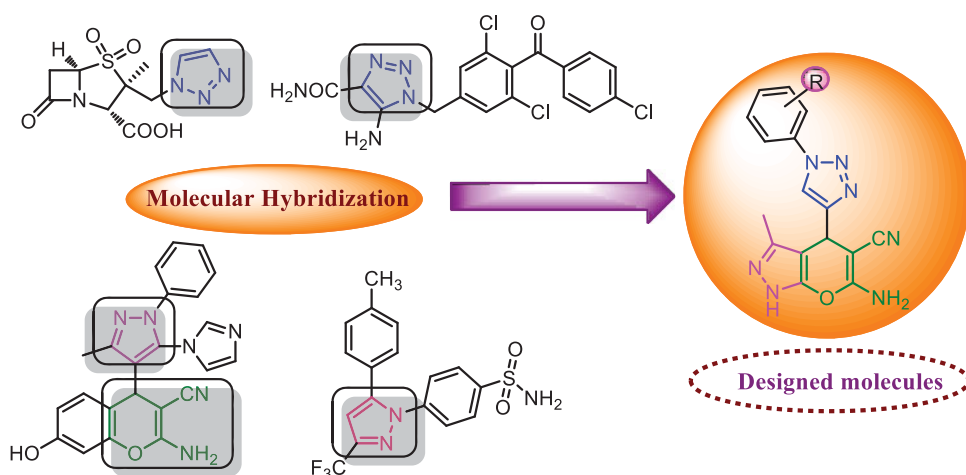


Figure 5. Designing of 1,2,3-triazolyl pyrano[2,3-c]pyrazoles by molecular hybridization approach.

compounds,^[28] we report herein the design and synthesis of a series of 1,2,3-triazolyl pyrano[2,3-c]pyrazoles which showed potent antifungal and antioxidant activities. The designing of the target scaffold is based on molecular hybridization strategy.^[29] We assembled the three biologically active scaffolds, i.e. 1,2,3-triazole, pyrazole, and 4*H*-pyran into a single molecular framework hopefully enhance the biological activity of the target scaffold (Figure 5).

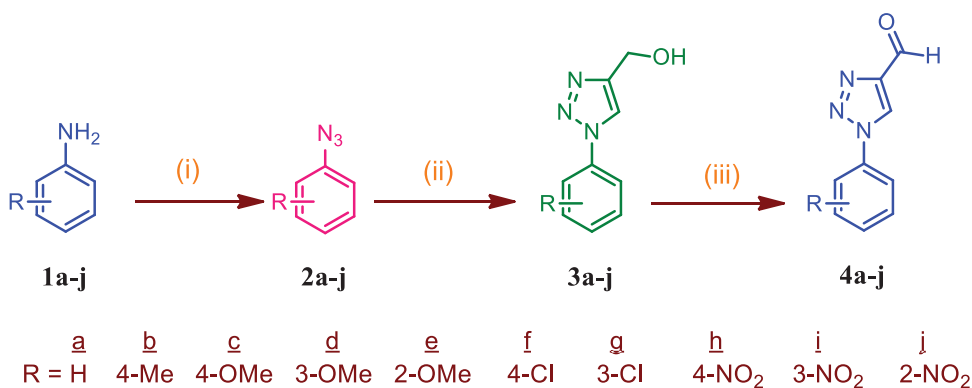
Results and discussion

Chemistry

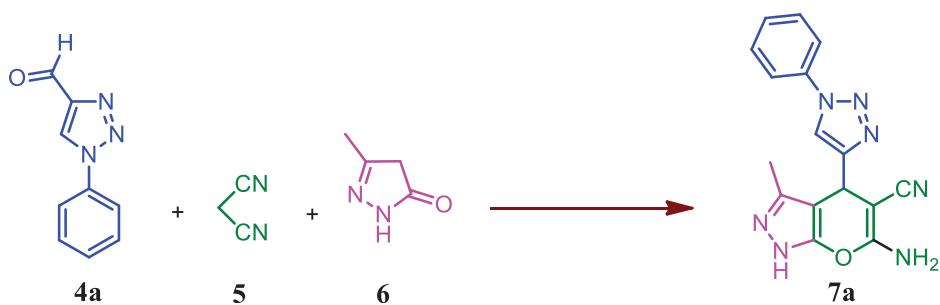
We have carried out the one-pot three-component synthesis of new 1,2,3-triazolyl pyrano[2,3-c]pyrazoles on the basis of molecular hybridization approach. Initially, the triazolyl aldehydes (**4a–j**) were prepared according to the reported method,^[30a] from the commercially available anilines (**1a–j**) by click chemistry approach (Scheme 1).

On the basis of successful applications of triazolyl aldehydes for the synthesis of various biologically active heterocyclic scaffolds,^[30] we have attempted the one-pot three-component synthesis of triazolyl pyrano[2,3-c]pyrazoles. At first, to optimize reaction conditions for the synthesis of triazolyl pyrano[2,3-c]pyrazole derivatives, the reaction of triazolyl aldehyde (**4a**), malononitrile (**5**) and pyrazolone (**6**) were chosen as a model reaction (Scheme 2). For this, pyrazolone **6** was prepared *in situ* by the condensation reaction of ethyl acetoacetate and hydrazine hydrate without any catalyst.

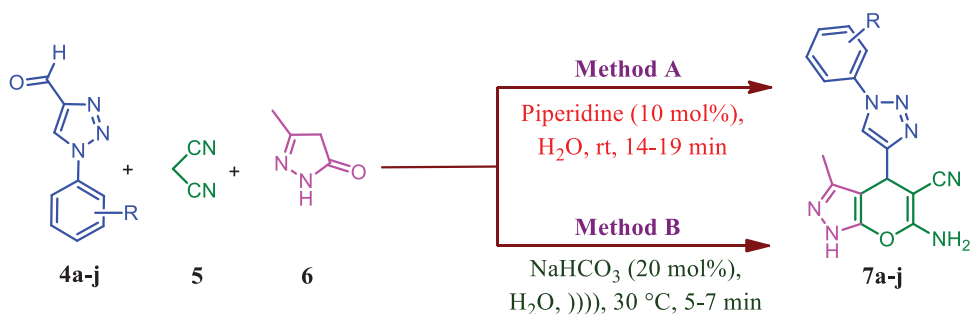
In our initial attempt, we have performed the model reaction by using piperidine (10 mol%) as a base in water and the reaction was carried at room temperature for 16 min (Scheme 2) (as per the reported method). The corresponding 1,2,3-triazolyl pyrano[2,3-c]pyrazole, **7a** was obtained in 84% yield. Furthermore, under the similar reaction conditions, the reaction of various triazolyl aldehydes (**4b–j**) was performed and obtained the corresponding 1,2,3-triazolyl pyrano[2,3-c] pyrazole derivatives (**7a–j**) in 80–92% yield (Scheme 3, Table 1, Method A). It is observed that the results were not satisfactory. Despite the reaction rate being fast, the yields were 80–92%.



Scheme 1. Synthetic route for triazolyl aldehydes (**4a-j**). Reagents and conditions: (i) NaNO₂, HCl (10%); NaN₃, 1–2 h, 0 °C; (ii) propargyl alcohol, CuSO₄·5H₂O, sodium ascorbate, *tert*-BuOH-H₂O (1:1), 24–48 h, rt; (iii) Collins reagent (CrO₃·2Py, CH₂Cl₂), 3–6 h, rt.



Scheme 2. Model reaction.



Scheme 3. Synthesis of 1,2,3-triazolyl pyrano[2,3-*c*]pyrazole derivatives (**7a-j**).

To elaborate greener synthetic protocol and to optimize reaction conditions for the synthesis of same 1,2,3-triazolyl pyrano[2,3-*c*]pyrazole derivatives **7a-j**, the model reaction (Scheme 2) was performed using various inorganic bases such as K₂CO₃, Na₂CO₃ and NaHCO₃ in water as a solvent under ultrasonic irradiation (40 kHz) at 30 °C and the results were summarized in Table 2. At the preliminary stage, the model reaction was carried out in the absence of catalyst under the same reaction parameters; it was observed that the desired product **7a** was not obtained even after prolonged reaction time (Table 2, entry 1). In our next attempt, the model reaction was performed by using

Table 1. Three component synthesis of 1,2,3-triazolyl pyrano[2,3-*c*]pyrazole derivatives (**7a–j**)^a.

Product	<i>R</i>	Method A		Method B	
		Time (min)	Yield ^b (%)	Time (min)	Yield ^b (%)
7a	H	16	84	7	98
7b	4-Me	15	86	5	97
7c	4-OMe	13	90	5	95
7d	3-OMe	14	88	4	92
7e	2-OMe	15	92	5	94
7f	4-Cl	14	88	4	98
7g	3-Cl	15	85	6	94
7h	4-NO ₂	17	82	4	93
7i	3-NO ₂	19	80	5	96
7j	2-NO ₂	15	84	5	92

^aReaction conditions: Method A: **4(a–j)** (1 mmol), **5** (1 mmol) and **6** (1 mmol), Piperidine (10 mol%), water (5 mL), rt. Method B: **4(a–j)** (1 mmol), **5** (1 mmol) and **6** (1 mmol), NaHCO₃ (20 mol%), water (5 mL), Ultrasonic irradiation (40 kHz), 30 °C;

^bIsolated yield.

Table 2. Optimization of the reaction conditions for the preparation of **7a**^a.

Entry	Catalyst	Amount of catalyst (mol%)	Time (min)	Yield (%) ^b
1	None	-	60	-
2	K ₂ CO ₃	10	30	80
3	K ₂ CO ₃	20	30	84
4	Na ₂ CO ₃	10	30	82
5	Na ₂ CO ₃	20	30	88
6	NaHCO ₃	10	10	88
7	NaHCO ₃	5	10	84
8	NaHCO ₃	15	10	96
9	NaHCO ₃	20	10	99
10	NaHCO ₃	25	10	99
11	NaHCO ₃	20	20	99
12	NaHCO ₃	25	20	99
13	NaHCO ₃	20	10	Trace ^c

^aReaction conditions: **4a** (1 mmol), **5** (1 mmol), and **6** (1 mmol), catalyst, water (5 mL), Ultrasonic irradiation (40 kHz), 30 °C;

^bIsolated yields;

^cWithout ultrasonic irradiation.

K₂CO₃ (10 and 20 mol%) under the similar reaction parameters, the desired product **7a** was obtained in 80 and 84% yield, respectively (Table 2, entries 2–3). Furthermore, the product **7a** was obtained in 82 and 88% yield with the use of 10 and 20 mol% of Na₂CO₃, respectively (Table 2, entry 4–5).

With the use of NaHCO₃ (10 mol%), the desired product **7a** was obtained in excellent yield (88%) in shorter reaction time (Table 2, entry 6). Therefore, it was observed that, among the screened inorganic bases, NaHCO₃ has been found to be an efficient catalyst in terms of time and yield. Further, to determine the optimal amount of NaHCO₃, the model reaction was subsequently tested for different concentrations, viz. 5, 15, 20 and 25 mol% (Table 2, entries 7–12). Using less than 20 mol% of NaHCO₃, the product **7a** was obtained in good yield (88–96%) (Table 2, entries 6–8). It was evident that 20 mol% of NaHCO₃ was sufficient to carry out the reaction in short reaction time with 99% yield (Table 2, entry 9). No further improvement in the yield was observed with 25 mol% of NaHCO₃ (Table 2, entry 10). However, no further increase in the yield was observed by using 20 and 25 mol% of the catalyst with extended reaction time (Table 1, entries 11–12). Finally, to examine the role of ultrasound, the model reaction was

performed without ultrasonic irradiation in presence of 20 mol% NaHCO₃ at 30 °C (Table 2, entry 13) and it was observed that the trace amount of desired product was obtained. In summary, the best results were obtained with 20 mol% of NaHCO₃ in water under ultrasonic irradiation (40 kHz) at 30 °C. These results signify that along with the catalyst, ultrasonic irradiation helps to improve the yield of the product in short reaction time.

The formation of the compound **7a** was confirmed by IR, ¹H NMR, ¹³C NMR, and mass analysis. The IR spectrum of **7a** displayed the absorption band at 3203 and 2189 cm⁻¹ due to the NH₂ and CN groups. The ¹H NMR spectrum of compound **7a** exhibited singlet peaks at δ 4.94, 7.00, 8.67, and 12.17 ppm due to the corresponding methine, -NH₂, triazolyl, and pyrazolyl protons. The ¹³C NMR spectrum of compound **7a** showed a peak at δ 28 ppm due to the stereogenic methine carbon of the 4*H*-pyran ring. In the mass spectrum of the compound **7a**, molecular ion peak observed at 320 corresponding to the calculated for C₁₆H₁₅N₇O ([M + H]⁺ 320.1260).

With these optimized reaction conditions in hand, the three component reaction of various substituted triazolyl aldehydes (**4b-j**), malononitrile (**5**), and pyrazolone (**6**) was investigated for the preparation of 1,2,3-triazolyl pyrano[2,3-*c*]pyrazole derivatives under the optimized reaction conditions (Scheme 3) and the obtained results were summarized in Table 1 (Method B). The reaction conditions work smoothly for electron donating and withdrawing groups (-Me, -OMe, -Cl, and -NO₂) on triazolyl aldehydes and corresponding products were obtained in good to excellent yields within shorter reaction time.

Biological assay

In vitro antifungal activity

In vitro antifungal activity of all the compounds, **7a-j** were evaluated against five human pathogenic fungal strains namely *Candida albicans* (NCIM 3471), *Fusarium oxysporum* (NCIM 1332), *Aspergillus flavus* (NCIM 539), *Aspergillus niger* (NCIM 1196), and *Cryptococcus neoformans* (NCIM 576). Minimum inhibitory concentration (MIC) values were determined by the standard agar dilution method. DMSO was used as solvent control. The results are compared with standard antifungal drug Miconazole and are illustrated in Table 3. It is observed from Table 3 that, most of the newly synthesized hybrids exhibited good to excellent antifungal activity against nearly all the tested fungal strains.

Among the 1,2,3-triazolyl pyrano[2,3-*c*]pyrazole derivatives (**7a-j**), compounds **7c**, **7d**, **7e**, **7f**, and **7i** display prominent antifungal activity against most of the tested fungal strains. Compound **7i** exhibited excellent antifungal activity with MIC = 12.5 µg/mL and found to be more potent than Miconazole against *C. albicans*. The compounds **7c** and **7e** were found to be equipotent to Miconazole against *C. albicans* with MIC = 25 µg/mL. Compounds **7d** and **7f** were exhibited equivalent activity compared to the standard drug against *F. oxysporum* with MIC = 25 µg/mL. It is promising to note that only the compound **7i** exhibited equivalent activity as compared to Miconazole with MIC = 25 µg/mL against *A. niger*. The compound **7f** exhibited equipotent activity compared to Miconazole against *C. neoformans* with MIC = 25 µg/mL. From Table 3, it is

Table 3. *In vitro* antifungal and antioxidant activity of synthesized compounds **7a–j**.

Compound	Antifungal activity (MIC) in $\mu\text{g/mL}$					Antioxidant activity IC_{50} ($\mu\text{g/mL}$)
	CA	FO	AF	AN	CN	
7a	62.5	87.5	50	100	62.5	27.17 ± 0.74
7b	50	75	25	75	50	21.08 ± 0.37
7c	25	50	25	75	50	14.77 ± 0.57
7d	37.5	25	37.5	50	50	11.07 ± 0.09
7e	25	50	50	100	50	09.39 ± 0.42
7f	50	25	75	50	25	12.91 ± 0.43
7g	175	175	200	175	150	19.11 ± 0.77
7h	137.5	125	200	150	125	14.97 ± 0.24
7i	12.5	50	25	25	75	11.99 ± 0.87
7j	175	200	*	150	*	10.22 ± 0.54
Miconazole	25	25	12.5	25	25	NT
BHT	NT	NT	NT	NT	NT	16.47 ± 0.18

CA: *Candida albicans*; FO: *Fusarium oxysporum*; AF: *Aspergillus flavus*; AN: *Aspergillus niger*; CN: *Cryptococcus neoformans*; BHT: butylated hydroxy toluene. *No activity up to 200 $\mu\text{g/mL}$; NT: Not tested.

observed that the antifungal activity varies with the substituent present on an aromatic unit of 1,2,3-triazolyl pyrano[2,3-*c*]pyrazole (**7a–j**). Compounds substituted with R = 4-OMe, 3-OMe, 2-OMe, 4-Cl, and 3-NO₂ exhibited excellent antifungal activity than the compounds substituted with R = H, 4-Me, 3-Cl, 4-NO₂, and 2-NO₂.

Antioxidant activity

The newly synthesized 1,2,3-triazolyl pyrano[2,3-*c*]pyrazole derivatives were evaluated for their *in vitro* antioxidant activity. The antioxidant activity results of the derivatives **7a–j** were obtained by using DPPH radical scavenging assay. Radical scavenging activity was measured in terms of IC_{50} value. Radical scavenging activity of all the compounds was compared with butylated hydroxyl toluene (BHT) having an IC_{50} value $16.47 \pm 0.18 \mu\text{g/mL}$ and the results were summarized in Table 3. Among the 1,2,3-triazolyl pyrano[2,3-*c*]pyrazoles (**7a–j**), it is promising to note that most of the compounds are excellent antioxidant agents than BHT. Compound **7e** exhibited excellent activity with appreciably lower IC_{50} value $09.39 \pm 0.42 \mu\text{g/mL}$ and found to be more potent than BHT. Compounds **7c**, **7d**, **7f**, **7h**, **7i**, and **7j** were found to be more potent than BHT with an IC_{50} values 14.77 ± 0.57 , 11.07 ± 0.09 , 12.91 ± 0.43 , 14.97 ± 0.24 , 11.99 ± 0.87 , and $10.22 \pm 0.54 \mu\text{g/mL}$, respectively.

Computational study

Molecular docking

In an effort to elucidate the possible mechanism by which the title compounds can induce antifungal activity and guide further SAR studies, molecular docking was performed into the active site of a crucial fungal target-sterol 14 α -demethylase (CYP51) inhibition of which prevents the conversion of lanosterol to ergosterol and subsequent accumulation of 14 α -methyl sterols in the cell leading to impaired cell growth in fungi. This *in silico* approach has now become an integral part of drug discovery pipeline, especially in the absence of available resources to carry out the enzymatic assays, imparting knowledge on binding affinities, binding modes and the associated

thermodynamic interactions with the target enzyme governing the inhibition of the causative pathogen. It is observed that all the ligands (**7a–7j**) showed similar orientation in the CYP51 active site and their complex formed was stabilized by the formation of several bonded and non-bonded interactions. Even their binding energies signifying the binding affinity were observed to be negative (–48.562 to –27.249 kcal/mol) while the average docking score was seen to be –7.271 kcal/mol. An in-depth investigation of the per-residue interaction between these compounds and the residues in the active site of the enzyme has been carried out to identify the most prominently interacting residues and their type of thermodynamic interactions (bonded and non-bonded interactions) that is critical in lead optimization. This analysis is discussed in detail for the most active 1,2,3-triazolyl pyrano[2,3-*c*]pyrazole derivative (**7i**) and the results are summarized in [Table 4](#) for the remaining molecules in the series.

Visual inspection and per-residue interaction analysis for the lowest energy docked conformation of active analogues **7i** showed that they could snugly fit into the active site of CYP51 at the same coordinates as the native ligand with a significantly higher binding affinity (docking score of –9.028 and Glide binding energy of –48.562 kcal/mol, respectively) engaging in a series of steric and electrostatic interactions ([Figure 6](#)).

Compound **7i** was observed to be stabilized in the active site of CYP51 through a series of significant van der Waals and electrostatic interactions. However, the most noticeable interactions are the hydrogen bonding interaction observed for **7i** with Met358 (2.04Å) through the pyrazole ring. Though **7i** did not engage in hydrogen bonding with Tyr103 (2.262Å) and Tyr116 (2.32Å) but it showed a very prominent π – π stacking interaction with these residues. The interactions with these three residues –Met358, Tyr103, and Tyr116 were consistently observed in all the active molecules in the series signifying their role in lead optimization. Such hydrogen bonding and π – π stacking interactions serve as an anchor for guiding the orientation of the ligand in the 3D space of the active site and facilitate the non-bonded (steric and electrostatic) interactions for stabilizing the enzyme-inhibitor complex. Further, **7i** was found to be engaged in a series of significant van der Waals interactions with residues lining the active site of CYP51; for **7i** with Hem500 (–6.375 kcal/mol), Phe290 (–1.485 kcal/mol), Ala287 (–1.614 kcal/mol), Met123 (–1.930 kcal/mol), Tyr116 (–2.186 kcal/mol), Ala115 (–1.962 kcal/mol), and Phe110 (–2.321 kcal/mol) residues through 6-amino-3-methyl-4-1-(3-nitrophenyl)-1*H*-1,2,3-triazol-4-yl component while the 1,4-dihydropyrano[2,3-*c*]pyrazole-5-carbonitrile component of the molecule interacted with Val461 (–2.107 kcal/mol), Met460 (–2.308 kcal/mol), Val359 (–2.401 kcal/mol), Leu356 (–2.151 kcal/mol), Ala291 (–2.938 kcal/mol), Tyr103 (–2.942 kcal/mol) residues. The higher binding observed for **7i** also attributed to a relatively fewer but significant electrostatic interactions as well observed with Hem500 (–4.406 kcal/mol), Cys422 (–2.656 kcal/mol), Arg361 (–1.038 kcal/mol), Met358 (–2.382 kcal/mol), Ala291 (–1.935 kcal/mol), Arg124 (–1.602 kcal/mol), and Arg100 (–1.362 kcal/mol) residues for **7i**. A similar network of bonded and non-bonded interactions was involved in stabilizing other molecules of the series into the active site CYP51 ([Figures S1–S9 Electronic Supplementary Information](#)). Furthermore, it is noteworthy that all the molecules in the series were seen to be engaged in a very strong van der Waals as well as electrostatic interactions with Heme moiety present in the active site of CYP51 which is an important observation



Table 4. Quantitative per-residue interaction analysis of the molecular docking study on sterol 14 α -demethylase (CYP51) for the 1,2,3-triazolyl pyrano[2,3-*c*]pyrazole derivatives.

Code	Docking Score	Glide Interaction Energy (kcal/mole)	Per-Residues interactions				π - π Stacking (Å)		
			Van der Waals (kcal/mol)	Coulombic (kcal/mol)	H-bonds(Å)				
7a	-6.967	-40.013	Hem500 (-5.911), Val461 (-1.637), Met460 (-1.407), Thr459 (-1.024), Met358 (-1.168), Leu356 (-1.114), Ala291 (-1.229), Phe290 (-1.377), Ala287 (-1.762), Leu127 (-1.029), Tyr116 (-1.862), Phe110 (-1.452), Met106 (-1.269), Tyr103 (-1.958), Hem500 (-6.068), Val461 (-1.994), Met460 (-2.101), Val359 (-1.759), Leu356 (-2.291), Ala291 (-1.951), Phe290 (-1.964), Ala287 (-1.911), Leu127 (-1.107), Tyr116 (-1.334), Phe110 (-1.717), Met106 (-1.919), Tyr103 (-1.021)	Hem500 (-4.577), Cys422 (-2.188), Met358 (-2.741)	Met358 (1.95)	Tyr103 (2.268), Tyr116 (2.615), Phe110 (2.701)			
			-44.807	Hem500 (-4.348), Cys422 (-1.879), Met358 (-1.184)	Met358 (2.13)	Tyr103 (1.991), Tyr116 (2.643)			
				-43.748	Hem500 (-6.335), Val461 (-2.086), Met460 (-2.057), Val359 (-1.831), Leu356 (-2.144), Thr295 (-1.554), His294 (-1.887), Ala291 (-2.278), Phe290 (-2.054), Ala288 (-1.169), Ala287 (-2.348), Leu127 (-1.057), Tyr116 (-2.031), Phe110 (-1.789), Met106 (-2.434), Tyr103 (-2.15)	Hem500 (-4.577), Cys422 (-2.313), Met358 (-2.531)	Met358 (2.03)	Tyr103 (2.104), Tyr116 (2.659)	
					-32.871	Hem500 (-5.511), Val461 (-1.776), Met460 (-1.919), Thr459 (-1.954), Leu356 (-2.136), His294 (-1.988), Ala291 (-2.467), Phe290 (-1.552), Ala288 (-1.654), Ala287 (-2.045), Leu127 (-1.213), Tyr116 (-4.341), Phe110 (-2.789), Tyr103 (-2.932), Hem500 (-5.61), Val461 (-2.166), Met460 (-2.374), Val359 (-1.25), Leu356 (-2.058), Ala291 (-1.991), Phe290 (-1.427), Ala287 (-1.074), Leu127 (-1.011), Tyr116 (-2.107), Phe110 (-1.661), Met106 (-2.151), Tyr103 (-2.084)	Hem500 (-4.348), Cys422 (-1.108), Met358 (-2.143)	Met358 (2.16)	Tyr103 (2.202), Tyr116 (2.586)
						-7.245	Hem500 (-4.577), Cys422 (-1.085), Met358 (-2.277)	Met358 (1.84)	Tyr103 (2.178), Tyr116 (2.629)

(continued)

Table 4. Continued.

Code	Docking Score	Glide Interaction Energy (kcal/mole)	Per-Residues interactions				π - π Stacking (Å)
			Van der Waals (kcal/mol)	Coulombic (kcal/mol)	H-bonds(Å)		
7f	-7.143	-42.983	Hem500 (-5.335), Val461 (-2.015),	Hem500 (-4.348),	Met358 (1.89)	Tyr103 (2.145), Tyr116 (2.747)	
			Met460 (-1.972), Val359 (-1.743),	Cys422 (-2.391),			
			Leu356 (-2.516), Ala291 (-2.568),	Met358 (-2.967)			
			Phe290 (-2.149), Ala287 (-2.102),				
			Tyr116 (-1.882), Phe110 (-1.726),				
			Met106 (-2.228)				
7g	-6.994	-40.051	Hem500 (-5.856), Val461 (-1.685),	Hem500 (-4.632),	Met358 (1.83)	Tyr103 (2.031)	
			Met460 (-1.275), Val359 (-1.202),	Met358 (-3.349),			
			Leu356 (-1.683), Ala291 (-1.918),	Arg233 (-1.15),			
			Phe290 (-1.433), Leu127 (-1.396),	Tyr116 (-1.015),			
			Tyr116 (-1.992), Phe110 (-1.177),				
			Met106 (-1.492), Tyr103 (-1.961)				
7h	-6.528	-29.686	Hem500 (-5.163), Val461 (-1.507),	Hem500 (-4.674),	Ala291 (1.82)	Tyr103 (2.473), Tyr116 (2.842)	
			Val359 (-1.156), Leu356 (-1.243),	Arg361 (-1.578),			
			Thr295 (-1.542), Ala288 (-1.762), 284	Ala291 (-1.529),			
			(-1.873), Tyr116 (-1.578), 115	Ala287 (-1.191),			
			(-1.356), Phe110 (-1.311), Met106	Glu205 (-1.593),			
			(-1.503), Tyr103 (-1.283)	Arg124 (-1.016)			
7i	-9.028	-48.562	Hem500 (-6.375), Val461 (-2.107),	Hem500 (-4.406),	Met358 (2.04)	Tyr103 (2.262), Tyr116 (2.32)	
			Met460 (-2.308), Val359 (-2.401),	Cys422 (-2.656),			
			Leu356 (-2.151), Ala291 (-2.938),	Arg361 (-1.038),			
			Phe290 (-1.485), Ala287 (-1.614),	Met358 (-2.382),			
			Met123 (-1.930), Tyr116 (-2.186),	Ala291 (-1.935),			
			Ala115 (-1.962), Phe110 (-2.321),	Arg124 (-1.602),			
7j	-6.291	-27.249	Tyr103 (-2.942)	Arg100 (-1.362)	Met358 (1.84)	Tyr103 (2.022), Tyr116 (2.165), Phe110 (2.019)	
			Hem500 (-4.651), Val461 (-1.313),	Hem500 (-4.189),			
			Met460 (-1.379), Val359 (-1.249),	Met358 (-1.294)			
			Leu356 (-1.555), Ala291 (-1.999),				
			Phe290 (-1.445), Ala287 (-1.043),				
			Tyr116 (-1.592), Phe110 (-1.681),				
Met106 (-1.629), Tyr103 (-1.961)							

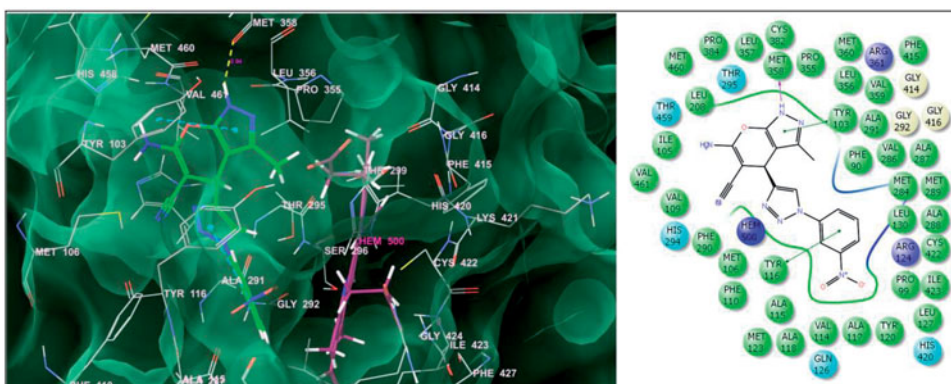


Figure 6. Binding mode of **7i** into the active site of sterol 14 α -demethylase (CYP51) (on right side: green lines signify π - π stacking interactions while the pink lines represent the hydrogen bonding interactions).

Table 5. Pharmacokinetic parameters of all synthesized compounds using *in silico* ADME prediction.

Entry	% ABS	TPSA	MV	MW	milog <i>p</i>	<i>n</i> -ON	<i>n</i> -OHNH	Lipinski's violations	<i>n</i> -ROTB	Drug likeness model score
Rule				<500	≤5	≤10	≤5	≤1		
7a	68.21	118.45	271.84	319.33	0.87	8	3	0	2	-0.12
7b	68.21	118.45	288.40	333.36	1.32	8	3	0	2	-0.55
7c	64.96	127.68	297.39	349.35	0.93	9	3	0	3	-0.33
7d	64.96	127.68	297.39	349.35	1.12	9	3	0	3	-0.21
7e	64.96	127.68	297.39	349.35	1.09	9	3	0	3	-0.26
7f	68.14	118.45	285.38	353.77	1.55	8	3	0	2	-0.02
7g	68.14	118.45	285.38	353.77	1.74	8	3	0	2	-0.20
7h	52.33	164.27	295.18	364.32	0.83	11	3	1	3	-0.40
7i	52.33	164.27	295.18	364.32	1.02	11	3	1	3	-0.32
7j	52.33	164.27	295.18	364.32	0.99	11	3	1	3	-0.34

considering the fact that Fluconazole is as well coordinated in the active site of CYP51 through the iron metal indicating that the title compounds may also share a similar mechanism for their anti-fungal action as Fluconazole. Overall, the information derived from the per-residue ligand interaction analysis could be fruitfully utilized for the structure-based lead optimization to arrive at potent antifungal agents with this scaffold.

***In silico* ADME prediction**

The success of drug depends upon its good efficacy, oral bioavailability, and ADME (absorption, distribution, metabolism, and excretion) properties. We have performed a computational study of all the compounds for the prediction of ADME properties. In this study, we have calculated molecular volume (MV), molecular weight (MW), log of partition coefficient (mi log *p*), number of hydrogen bond donors (*n*-ON), number of hydrogen bond acceptors (*n*-OHNH), topological polar surface area (TPSA), number of rotatable bonds (*n*-ROTB) and Lipinski's rule of five^[31] using the molinspiration online property calculation toolkit (Molinspiration Cheminformatics, Slovak Republic).^[32] Absorption (%ABS) was calculated by the formula $\%ABS = 109 - (0.345 \times TPSA)$.^[33]

The obtained results of ADME prediction are presented in Table 5. It is observed that the compounds exhibited good absorption (%ABS) ranging between 52–68%. Moreover, most of the compounds show good agreement with Lipinski's rule of five. The drug-likeness model score, the collective property of physicochemical properties was also calculated by using MolSoft software.^[34] Thus, most of the derivatives possess the good potential to be developed as an orally active drug molecule.

Conclusions

In conclusion, novel 1,2,3-triazolyl pyrano[2,3-*c*]pyrazole derivatives have been synthesized through a one-pot multicomponent reaction (MCR) approach using NaHCO₃ as a catalyst under ultrasonic irradiation in excellent yield. All the compounds were evaluated against five pathogenic fungal strains and results showed that the compound **7i** found to be more potent than Miconazole against *Candida albicans*. Compounds **7c**, **7d**, **7e**, and **7f** exhibited excellent antifungal activity and equipotent to Miconazole. Furthermore, all the compounds were also investigated for their *in vitro* antioxidant activity and most of them found to be more potent than BHT with a lower IC₅₀ value (IC₅₀ < 16.49 ± 0.44). Molecular docking studies against a target enzyme sterol 14 α -demethylase (CYP51) showed a significant correlation between binding score and antifungal activity. *In silico* ADME properties prediction reveals, most of the compounds can be developed as lead candidates. Thus, the results suggest that 1,2,3-triazolyl pyrano[2,3-*c*]pyrazoles can open new opportunities for antifungal and antioxidant agents in further clinical research.

Experimental

General

All the solvents and reagents were purchased from commercial suppliers Spectrochem Pvt. Ltd., Sigma Aldrich and Rankem India Ltd. and used without further purification. All the one-pot reactions were performed using citizen (CUB 2.5, Mumbai, India) ultrasonic cleaner bath working at 40 kHz (constant frequency, 50 W). The progress of each reaction was monitored by ascending thin layer chromatography (TLC) using TLC aluminum sheets, silica gel 60 F₂₅₄ precoated, Merck, Germany and locating the spots using UV light as the visualizing agent or iodine vapors. Melting points were determined in open capillary method and are uncorrected. Infrared (IR) spectra were recorded on a Bruker FT-IR spectrometer. ¹H NMR spectra were recorded (CDCl₃/DMSO-*d*₆) on Bruker Avance 200 and 500 MHz NMR spectrometer (Bruker, Billerica, MA). ¹³C NMR spectra were recorded (CDCl₃/DMSO-*d*₆) on Bruker Avance 50 and 125 MHz NMR spectrometer. Mass spectra were recorded on an Agilent 6520 (Q-Tof) (ESI-HRMS) (Agilent, Santa Clara, CA) and Waters UPLC-TQD (ESI-MS) instrument (Waters Corporation, Milford, MA). The elemental analysis values were recorded on Thermofisher FA-2001 CHNS analyzer. Chemical shifts (δ) are reported in parts per million (ppm) using tetramethylsilane (TMS) as an internal standard. The splitting pattern abbreviations are designed as singlet (s); doublet (d); double doublet (dd); triplet (t) and multiplet (m).

General procedure for the synthesis of 1,2,3-triazolyl pyrano[2,3-c]pyrazoles (7a–j)

Method A

A mixture of 1-aryl-1H-1,2,3-triazole-4-carbaldehyde (**4a–j**) (1 mmol), malononitrile (**5**) (1 mmol), pyrazolone **6** (1 mmol) and piperidine (10 mol%) in water (5 mL) was taken in 50 mL round bottom flask and the mixture was stirred at room temperature for appropriate time. After the completion of the reaction (monitored by TLC), the reaction mixture was poured into 20 mL ice-water and the obtained solid was filtered, washed thoroughly with water, dried, and recrystallized from ethanol to afford the pure products (**7a–j**).

Method B

A mixture of 1-aryl-1H-1,2,3-triazole-4-carbaldehyde (**4a–j**) (1 mmol), malononitrile (**5**), (1 mmol) pyrazolone **6** (1 mmol), and NaHCO₃ (20 mol%) in water (5 mL) was taken in 50 mL round bottom flask and the mixture was sonicated in an ultrasonic bath working at 40 kHz (constant frequency) at 30 °C for appropriate time. After the completion of the reaction (monitored by TLC), the reaction mixture was poured into 20 mL ice-water and the obtained solid was filtered, washed thoroughly with water, dried and recrystallized from ethanol to afford the pure products (**7a–j**) in excellent yields.

6-Amino-3-methyl-4-(1-phenyl-1H-1,2,3-triazol-4-yl)-1,4-dihydropyrano[2,3-c]pyrazole-5-carbonitrile (7a)

Mp: 205–207 °C. IR ν_{max} (cm⁻¹): 3319, 3203 (–NH₂), 2189 (–CN), 1634 (C=C vinyl nitrile), 1587 (C=C–Aromatic). ¹H NMR (200 MHz, DMSO-*d*₆, δ ppm): 1.98 (s, 3H, –CH₃), 4.94 (s, 1H, methine), 7.00 (s, 2H, –NH₂), 7.43–7.62 (m, 3H), 7.93 (d, 2H, *J* = 8 Hz), 8.67 (s, 1H, triazolyl-H), 12.17 (s, 1H, pyrazolyl-H). ¹³C NMR (50 MHz, DMSO-*d*₆, δ ppm): 9.8, 28, 54.9, 96, 119.7, 120, 120.7, 128.5, 130, 136, 136.6, 151.3, 154.6, 161.3. ESI-MS: *m/z* 320 [M + H]⁺. Anal. Calcd. for C₁₆H₁₃N₇O: C, 60.18; H, 4.10; N, 30.70%; Found: C, 60.37; H, 4.11; N, 30.67%.

Supporting information PDF file contains an experimental protocol for biological activity and computational studies, and spectral data of compounds **7a–j** (FT-IR, ¹H and ¹³C NMR, mass and CHNS spectra) of the compounds.

Acknowledgments

One of the authors S. P. K. is grateful to Dr. Babasaheb Ambedkar Marathwada University, Aurangabad, for the award of University Scholars Fellowship. Authors are also thankful to the Head, Department of Chemistry, Dr. Babasaheb Ambedkar Marathwada University, Aurangabad, 431 004, Maharashtra, India, for providing laboratory facility. Authors also acknowledge Schrodinger Inc. for providing GLIDE software to perform the molecular modeling studies.

References

- [1] Enoch, D. A.; Ludlam, H. A.; Brown, N. M. *J. Med. Microbiol.* **2006**, *55*, 809–818. DOI: [10.1099/jmm.0.46548-0](https://doi.org/10.1099/jmm.0.46548-0).
- [2] Lai, C. C.; Tan, C. K.; Huang, Y. T.; Shao, P. L.; Hsueh, P. R. *J. Infect. Chemother.* **2008**, *14*, 77–85. DOI: [10.1007/s10156-007-0595-7](https://doi.org/10.1007/s10156-007-0595-7).
- [3] (a) Zhao, S.; Zhang, X.; Wei, P.; Su, X.; Zhao, L.; Wu, M.; Hao, C.; Liu, C.; Zhao, D.; Cheng, M. *Eur. J. Med. Chem.* **2017**, *137*, 96–107. DOI: [10.1016/j.ejmech.2017.05.043](https://doi.org/10.1016/j.ejmech.2017.05.043). (b) Andriole, V. T. *Int. J. Antimicrob. Agents* **2000**, *16*, 317–321.
- [4] Xu, K.; Huang, L.; Xu, Z.; Wang, Y.; Bai, G.; Wu, Q.; Wang, X.; Yu, S.; Y, J. *Drug Des. Dev. Ther.* **2015**, *9*, 1459–1467.
- [5] Agalave, S. G.; Maujan, S. R.; Pore, V. S. *Chem. Asian J.* **2011**, *6*, 2696–2718. DOI: [10.1002/asia.201100432](https://doi.org/10.1002/asia.201100432).
- [6] Jiang, Z.; Gu, J.; Wang, C.; Wang, S.; Liu, N.; Jiang, Y.; Dong, G.; Wang, Y.; Liu, Y.; Yao, J.; et al. *Eur. J. Med. Chem.* **2014**, *82*, 490–497. DOI: [10.1016/j.ejmech.2014.05.079](https://doi.org/10.1016/j.ejmech.2014.05.079).
- [7] Gill, C.; Jadhav, G.; Shaikh, M.; Kale, R.; Ghawalkar, A.; Nagargoje, D.; Shiradkar, M. *Bioorg. Med. Chem. Lett.* **2008**, *18*, 6244–6247. DOI: [10.1016/j.bmcl.2008.09.096](https://doi.org/10.1016/j.bmcl.2008.09.096).
- [8] Mareddy, J.; Suresh, N.; Kumar, C. G.; Kapavarapu, R.; Jayasree, A.; Pal, S. *Bioorg. Med. Chem. Lett.* **2017**, *27*, 518–523. DOI: [10.1016/j.bmcl.2016.12.030](https://doi.org/10.1016/j.bmcl.2016.12.030).
- [9] Abdel-Wahab, B. F.; Abdel-Latif, E.; Mohamed, H. A.; Awad, G. E. A. *Eur. J. Med. Chem.* **2012**, *52*, 263–268. DOI: [10.1016/j.ejmech.2012.03.023](https://doi.org/10.1016/j.ejmech.2012.03.023).
- [10] Wu, M.-J.; Wu, D.-M.; Chen, J.-B.; Zhao, J.-F.; Gong, L.; Gong, Y.-X.; Li, Y.; Yang, X.-D.; Zhang, H. *Bioorg. Med. Chem. Lett.* **2018**, *28*, 2543–2549. DOI: [10.1016/j.bmcl.2018.05.038](https://doi.org/10.1016/j.bmcl.2018.05.038).
- [11] Karypidou, K.; Ribone, S. R.; Quevedo, M. A.; Persoons, L.; Pannecouque, C.; Helsen, C.; Claessens, F.; Dehaen, W. *Bioorg. Med. Chem. Lett.* **2018**, *28*, 3472–3476. DOI: [10.1016/j.bmcl.2018.09.019](https://doi.org/10.1016/j.bmcl.2018.09.019).
- [12] Bi, F.; Ji, S.; Venter, H.; Liu, J.; Semple, S. J.; Ma, S. *Bioorg. Med. Chem. Lett.* **2018**, *28*, 884–891. DOI: [10.1016/j.bmcl.2018.02.001](https://doi.org/10.1016/j.bmcl.2018.02.001).
- [13] Li, J.-C.; Zhang, J.; Rodrigues, M. C.; Ding, D.-J.; Longo, J. P. F.; Azevedo, R. B.; Muehlmann, L. A.; Jiang, C.-S. *Bioorg. Med. Chem. Lett.* **2016**, *26*, 3881–3885. DOI: [10.1016/j.bmcl.2016.07.017](https://doi.org/10.1016/j.bmcl.2016.07.017).
- [14] (a) Schoonover, L. L.; Occhipinti, D. J.; Rodvold, K. A.; Danziger, L. H. *Ann. Pharmacother.* **1995**, *29*, 501–514. DOI: [10.1177/106002809502900510](https://doi.org/10.1177/106002809502900510). (b) Camarasa, M. J.; Velazquez, S.; San-Felix, A.; Perez-Perez, M. J.; Bonache, M. C.; De Castro, S. *Curr. Pharm. Des.* **2006**, *12*, 1895–1907. (c) Grover, G. J.; Kelly, J.; Moore, G.; Jacoby, H.; Karmali, R. A.; Gorman, G. S. *Cancer Ther.* **2007**, *5*, 437–442. (d) Yao, Z.; Li, J.; Liu, Z.; Zheng, L.; Fan, N.; Zhang, Y.; Jia, N.; Lv, J.; Liu, N.; Zhu, X.; et al. *Mol. BioSyst.* **2016**, *12*, 729–736.
- [15] Ansari, A.; Ali, A.; Asif, M.; Shamsuzzaman, S. *New J. Chem.* **2017**, *41*, 16–41. DOI: [10.1039/C6NJ03181A](https://doi.org/10.1039/C6NJ03181A).
- [16] Horrocks, P.; Pickard, M. R.; Parekh, H. H.; Patel, S. P.; Pathak, R. B. *Org. Biomol. Chem.* **2013**, *11*, 4891–4898. DOI: [10.1039/c3ob27290g](https://doi.org/10.1039/c3ob27290g).
- [17] Kumar, R. S.; Arif, I. A.; Ahamed, A.; Idhayadhulla, A. *Saudi J. Biol. Sci.* **2016**, *23*, 614–620. DOI: [10.1016/j.sjbs.2015.07.005](https://doi.org/10.1016/j.sjbs.2015.07.005).
- [18] Datar, P. A.; Jadhav, S. R. *Int. J. Med. Chem.* **2015**, *2015*, 670–679.
- [19] Ragavan, R. V.; Vijayakumar, V.; Kumari, N. S. *Eur. J. Med. Chem.* **2010**, *45*, 1173–1180. DOI: [10.1016/j.ejmech.2009.12.042](https://doi.org/10.1016/j.ejmech.2009.12.042).
- [20] Bekhit, A. A.; Hymete, A.; Asfaw, H.; El-Din, A.; Bekhit, A. *Arch. Pharm. (Weinheim)* **2012**, *345*, 147–154. DOI: [10.1002/ardp.201100078](https://doi.org/10.1002/ardp.201100078).
- [21] Kucukguzel, S. G.; Senkardes, S. *Eur. J. Med. Chem.* **2015**, *97*, 786–815. DOI: [10.1016/j.ejmech.201.11.059](https://doi.org/10.1016/j.ejmech.201.11.059).
- [22] (a) Sabry, N. M.; Mohamed, H. M.; Khattab, E. S. A. E. H.; Motlaq, S. S.; El-Agrody, A. M. *Eur. J. Med. Chem.* **2011**, *46*, 765–772. DOI: [10.1016/j.ejmech.2010.12.015](https://doi.org/10.1016/j.ejmech.2010.12.015). (b) Ren,

- Q.; Siau, W. Y.; Du, Z.; Zhang K.; Wang, J. *Chem. Eur. J.* **2011**, *17*, 7781–7785. DOI:10.1002/chem.201100927. (c) Shestopalov, A. M.; Litvinov, Y. M.; Rodinovskaya, L. A.; Malyshev, O. R.; Semenova, M. N.; Semeno, V. V. *ACS Comb. Sci.* **2012**, *14*, 484–490. DOI: 10.1021/co300062e. (d) Kalaria, P. N.; Sataasia, S. P.; Raval, D. K. *New J. Chem.* **2014**, *38*, 1512–1521. DOI: 10.1039/c3nj01327h. (e) Pratap, R.; Ram, V. J. *Chem. Rev.* **2014**, *114*, 10476–10526. DOI: 10.1021/cr500075s. (f) Chougala, B. M.; Samundeeswari, S.; Holiyachi, M.; Shastri, L. A.; Dodamani, S.; Jalalpure, S.; Dixit, S. R.; Joshi, S. D.; Sunagar, V. A. *Eur. J. Med. Chem.* **2017**, *125*, 101–116.
- [23] (a) Vasuki, G.; Kumaravel, K. *Tetrahedron Lett.* **2008**, *49*, 5636–5638. DOI: 10.1016/j.tetlet.2008.07.055. (b) Reddy, M. B. M.; Jayashankara, V. P.; Pasha, M. A. *Synth. Commun.* **2010**, *40*, 2930–2934. DOI: 10.1080/00397910903340686. (c) Moosavi-Zare, A. R.; Zolfigol, M. A.; Noroozizadeh, E.; Tavasoli, M.; Khakyzadeh, V.; Zare, A. *New J. Chem.* **2013**, *37*, 4089–4094. DOI: 10.1039/c3nj00629h. (d) Tamaddon, F.; Alizadeh, M. *Tetrahedron Lett.* **2014**, *55*, 3588–3591. DOI: 10.1016/j.tetlet.2014.04.122. (e) Alibeik, M. A.; Moaddeli, A.; Masoomi, K. *RSC Adv.* **2015**, *5*, 74932–74939. DOI: 10.1039/C5RA11343A. (f) Moosavi-Zare, A. R.; Zolfigol, M. A.; Mousavi-Tashar, A. *Res. Chem. Intermed.* **2016**, *42*, 7305–7312. DOI: 10.1007/s11164-016-2537-4. (g) Waghmare, A. S.; Pandit, S. S. *J. Saudi Chem. Soc.* **2017**, *21*, 286–290. DOI: 10.1016/j.jscs.2015.06.010. (h) Kumar Gangu, K.; Maddila, S.; Maddila, S. N.; Jonnalagadda, S. B. *RSC Adv.* **2017**, *7*, 423–432. DOI: 10.1039/C6RA25372E. (i) Reddy, G. M.; Garcia, J. R. *J. Heterocyclic Chem.* **2017**, *54*, 89–94.
- [24] (a) Aliabadi, R. S.; Mahmoodi, N. O. *RSC Adv.* **2016**, *6*, 85877–85884. DOI: 10.1039/C6RA17594E. (b) Esmailpour, M.; Javidi, J.; Dehghani, F.; Dodeji, F. N. *RSC Adv.* **2015**, *5*, 26625–26633. DOI: 10.1039/C5RA01021G. (c) Dekamin, M. G.; Eslami, M. *Green Chem.* **2014**, *16*, 4914–4921. DOI: 10.1039/C4GC00411F. (d) Qareaghaj, O. H.; Mashkouri, S.; Naimi-Jamal, M. R.; Kaupp, G. *RSC Adv.* **2014**, *4*, 48191–48201.
- [25] (a) Domling, A.; Ugi, I. *Angew. Chem. Int. Ed.* **2000**, *39*, 3168–3210. (b) Estevez, V.; Villacampa, M.; Menendez, J. C. *Chem. Soc. Rev.* **2014**, *43*, 4633–4657. DOI: 10.1039/c3cs60015g. (c) Levi, L.; Muller, T. J. *J. Chem. Soc. Rev.* **2016**, *45*, 2825–2846.
- [26] (a) Pirrung, M. C.; Sarma, K. D. *J. Am. Chem. Soc.* **2004**, *126*, 444–445. DOI: 10.1021/ja038583a. (b) Simon, M.-O.; Li, C.-J. *Chem. Soc. Rev.* **2012**, *41*, 1415–1427. DOI: 10.1021/ja038583a.
- [27] (a) Suslick, K. S.; Price, G. J. *Ann. Rev. Mater. Sci.* **1999**, *29*, 295. DOI: 10.1146/annurev.matsci.29.1.295. (b) Cravotto, G.; Cintas, P. *Chem. Soc. Rev.* **2006**, *35*, 180–196. DOI: 10.1039/b503848k. (c) Banerjee, B. *Ultrason. Sonochem.* **2017**, *35*, 15–35.
- [28] (a) Shaikh, M. H.; Subhedar, D. D.; Nawale, L.; Sarkar, D.; Khan, F. A. K.; Sangshetti, J. N.; Shingate, B. B. *Med. Chem. Commun.* **2015**, *6*, 1104–1116. DOI: 10.1039/C5MD00057B. (b) Subhedar, D. D.; Shaikh, M. H.; Shingate, B. B.; Nawale, L.; Sarkar, D.; Khedkar, V. M. *Med. Chem. Commun.* **2016**, *7*, 1832–1848. DOI: 10.1039/C6MD00278A. (c) Subhedar, D. D.; Shaikh, M. H.; Arkile, M. A.; Yeware, A.; Sarkar, D.; Shingate, B. B. *Bioorg. Med. Chem. Lett.* **2016**, *26*, 1704–1708. DOI: 10.1016/j.bmcl.2016.02.056. (d) Subhedar, D. D.; Shaikh, M. H.; Nawale, L.; Sarkar, D.; Khedkar, V. M.; Shingate, B. B. *Bioorg. Med. Chem. Lett.* **2017**, *27*, 922–928. DOI: 10.1016/j.bmcl.2017.01.004. (e) Subhedar, D. D.; Shaikh, M. H.; Shingate, B. B.; Nawale, L.; Sarkar, D.; Khedkar, V. M.; Khan, F. A. K.; Sangshetti, J. N. *Eur. J. Med. Chem.* **2017**, *125*, 385–399.
- [29] (a) Viegas-Junior, C.; Danuello, A.; da Silva Bolzani, V.; Barreiro, E. J.; Fraga, C. A. M. *Curr. Med. Chem.* **2007**, *14*, 1829–1852. (b) Maia, R.; do C.; Fraga, C. A. M. *Curr. Enzyme Inhib.* **2010**, *6*, 171–182.
- [30] (a) Danne, A. B.; Choudhari, A. S.; Chakraborty, S.; Sarkar, D.; Khedkar, V. M.; Shingate, B. B. *Med. Chem. Commun.* **2018**, *9*, 1114–1130. DOI: 10.1039/c8md00055g. (b) Khare, S. P.; Deshmukh, T. R.; Sangshetti, J. N.; Krishna, V. S.; Sriram, D.; Khedkar, V. M.; Shingate, B. B. *ChemistrySelect.* **2018**, *3*, 13113–13122. DOI: 10.1002/slct.201801859. (c) Danne, A. B.; Choudhari, A. S.; Sarkar, D.; Sangshetti, J. N.; Khedkar, V. M.; Shingate, B. B. *Res. Chem. Intermed.* **2018**, *44*, 6283–6310. DOI: 10.1007/s11164-018-3490-1. (d) Goud,

- G. L.; Ramesh, S.; Ashok, D.; Reddy, V. P.; Yogeeswari, P.; Sriram, D.; Saikrisna, B.; Manga, V. *Med. Chem. Commun.* **2017**, *8*, 559–570.
- [31] Lipinski, C. A.; Lombardo, F.; Dominy, B. W.; Feeney, P. J. *Adv. Drug Delivery Rev* **2001**, *46*, 3–26. DOI: [10.1016/S0169-409X\(00\)00129-0](https://doi.org/10.1016/S0169-409X(00)00129-0).
- [32] Molinspiration Chemoinformatics Bratislava, Slovak Republic, **2014**. <http://www.molinspiration.com/cgi-bin/properties> (accessed Jan 28, 2019).
- [33] Zhao, Y. H.; Abraham, M. H.; Le, J.; Hersey, A.; Luscombe, C. N.; Beck, G.; Sherborne, B.; Cooper, I. *Pharm. Res.* **2002**, *19*, 1446–1457. DOI: [10.1023/A:1020444330011](https://doi.org/10.1023/A:1020444330011).
- [34] Molsoft. Drug-likeness and molecular property prediction. <http://www.molsoft.com/mprop> (accessed Jan 28, 2019).